Available online at www.sciencedirect.com
SCIENCE DIRECT
Journal of Photochemistry and Photobiology A: Chemistry 181 (2006) 152–157
Journal of Photochemistry and Photobiology A:Chemistry
www.elsevier.com/locate/jphotochem

Electronic characterization and photocatalytic properties of CdS/TiO_2 semiconductor composite

Juliana C. Tristão [a], Fabiano Magalhães [a], Paola Corio [b], Maria Terezinha C. Sansiviero [a,*]

[a] *Departamento de Química, Instituto de Ciências Exatas, Universidade Federal de Minas Gerais, Av. Antônio Carlos, 6627, 3127-901 Belo Horizonte, MG, Brazil*
[b] *Instituto de Química, Universidade de São Paulo, Av. Prof. Lineu Prestes, 748, 05508-900 São Paulo, SP, Brazil*

Received 25 August 2005; received in revised form 16 November 2005; accepted 17 November 2005
Available online 28 December 2005

Abstract

Titanium dioxide is broadly used as a catalyst for photochemical reactions. In this work, nanometric particles of CdS (a narrow band gap semiconducting material) were used to impregnate TiO_2 in order to optimize its photocatalytic properties. CdS/TiO_2 semiconductor composites were obtained in 1, 3, 5 and 20 mol% proportion and characterized by differential thermogravimetric analysis (DTG), X-ray diffraction (XRD), laser-induced fluorescence (LIF) and resonance Raman spectroscopy. The results identified the CdS in hexagonal geometry and the TiO_2 in anatase form. Resonance Raman spectroscopy data revealed a lattice softening of the TiO_2-anatase phase due to electronic interaction between TiO_2 and CdS in the CdS/TiO_2 catalyst. The effect of modifying the proportion of CdS in the catalyst electronic properties and efficiency was also studied. The photocatalytic activity of the CdS/TiO_2 was investigated using artificial UV light for degradation of the textile azo-dye Drimaren red. The photocatalytic analysis revealed better efficiency for the CdS/TiO_2 5% composite as compared with other CdS/TiO_2 proportions and with TiO_2 alone.
© 2005 Elsevier B.V. All rights reserved.

Keywords: Photocatalysis; Resonance Raman; Titanium dioxide; Cadmium sulfide; Advanced oxidative processes; Environmental photochemistry

1. Introduction

Heterogeneous photocatalysis using the semiconductor titanium dioxide (TiO_2) is a general and efficient method for destroying organic pollutants in aqueous media, and its use has been increasing for the treatment of a number of industrial residues [1]. For instance, photocatalytic transformations of pesticides in aqueous TiO_2 suspensions using solar light were recently reviewed by Konstantinou and Albanis [2]. Such processes are based on the incidence of radiation on the semiconducting material. If the energy of the incident radiation is higher than the semiconducting band gap electrons are promoted from the valence band to the conduction band in other words, an electron–hole pair is produced. The catalytic effect on the degradation of organic compounds can be explained by the presence of this electron–hole pair in the semiconducting material. A disadvantage of the use of TiO_2 as a photocatalyst is due to its relatively large band gap ($E_g = 3.2$ eV for anatase phase): its efficiency depends on the presence of radiation with relatively low wavelength, in the ultra-violet spectral region. Due to this limitation, the preparation of photocatalysts that can be excited in the visible range is of great interest for the development of photocatalytic processes that use solar radiation for the degradation of organic pollutants. One promising approach is based on the association of TiO_2 with other semiconducting materials with lower band gaps. The preparation of many composite materials involving TiO_2 may be found in the recent literature, aiming at enhancement or modulation its catalytic properties. Some examples include the modification of TiO_2 with silver ions or oxides [3–5]. The capacity of coupled $CdSe/TiO_2$ for photocatalytic degradation of 4-chlorophenol has already been reported in the literature [6].

In this work, we associated TiO_2 with cadmium sulfide (CdS), a semiconductor material with a band gap in the vis-

* Corresponding author. Tel.: +55 31 3499 5763; fax: +55 31 3499 5700.
E-mail address: mtcaruso@netuno.lcc.ufmg.br (M.T.C. Sansiviero).

1010-6030/$ – see front matter © 2005 Elsevier B.V. All rights reserved.
doi:10.1016/j.jphotochem.2005.11.018

ible range (2.42 eV) [7,8]. Coupled TiO_2-based semiconductor systems have attracted much interest, partly because of synergistic effects on photoelectrochemical properties [8,9] and photocatalytic activity [10]. Recent literature includes several examples of studies of coupled CdS/TiO_2 systems. CdS/TiO_2 colloids have been studied in photoelectrochemistry and water splitting systems [11,12]. Photocatalytic properties of CdS/TiO_2 heterojunctions prepared by direct mixture of both constituents and by precipitation of the sensitizer with commercial TiO_2 were demonstrated under UV and visible light [13]. Bulk CdS mixed with TiO_2 particles was also developed for visible light photocatalysis [14]. Takahashi et al. [15] described photocatalytic activities and the morphology of particulate assemblies of CdS and TiO_2 prepared by Langmuir–Blodgett technique. It was verified that alternate CdS/TiO_2 particulate layer is less active for the oxidative decomposition. The possibility of transferring photoexcited electrons of CdS nanocrystals to the conduction band of TiO_2 was suggested by photocurrent studies of highly porous TiO_2 electrodes sensitized by quantum-sized CdS [16]. Photosensitization of titanium compounds (such as ion-exchangeable hollow titanate nanotubes and crystalline TiO_2) by CdS was also reported [17,18].

Nanometric particles of CdS were obtained from a single-source molecular precursor—cadmium thiourea [19,20]. The CdS/TiO_2 semiconductor composites were prepared in different mass proportions by the thermal decomposition of cadmium thiourea impregnated on TiO_2. Its photocatalytic activity was studied in the decomposition of a reactive textile dye Drimaren red (Clariant), and its performance was compared to pure TiO_2. The photocatalyst material was also characterized in terms of its structure (by means of thermogravimetric and X-ray diffractometry (XRD) techniques) and in terms of the electronic interaction between both semiconductors by resonance Raman spectroscopy and laser-induced fluorescence (LIF) techniques. Resonance Raman spectroscopy was particularly useful here, since it allows to investigate molecular or solid-state vibrations that are coupled to electronic transitions, and is a well-established probe of semiconductor materials [21].

2. Experimental

2.1. Materials and instrumentation

CdS/TiO_2 composites were characterized by differential thermogravimetric analysis (DTG), X-ray diffractometry, Raman spectroscopy and laser-induced fluorescence. The Raman spectra were acquired on a Renishaw Raman System 3000 equipped with a CCD detector and coupled to an Olympus microscope (BTH2) that allows a rapid accumulation of Raman spectra with a spatial resolution of about 1 μm (micro-Raman technique). The laser beam was focused on the sample by a ×80 lens. Laser power was always kept below 0.7 mW at the sample to avoid laser-induced sample degradation. The experiments were performed at ambient conditions using a back-scattering geometry. The samples were irradiated with the 632.8 nm line of a He–Ne laser (Spectra Physics) or 514.5 nm line of an Ar^+ laser. FT-Raman spectra of solid samples were recorded at room temperature in a RFS 100 FT-Raman Bruker spectrometer using the 1064.0 nm radiation from a Nd:YAG laser. The photoluminescence (PL) spectra were taken with the samples under vacuum inside an immersion cryostat. We have used a CW Ar-ion laser emitting at 488 nm as the excitation source. The PL emission was collected from the samples at 45° configuration, focused into a SPEX 0.75 m monochromator, and detected by a gallium arsenide (GaAs) photomultiplier tube. X-ray power diffraction patterns were recorded on a Rigaku Geigerflex equipment using nickel-filtered Cu Kα radiation (λ = 1.5418 Å) and a graphite monochromator in the diffracted beam. A scan rate of 4° min^{-1} was applied to record a pattern in the 2θ range of 2θ = 8–60°. Thermogravimetric analysis (TG and DTG) were carried out in a Shimadzu TGA 50H in nitrogen flow and heating rate of 10 °C min^{-1}.

Degussa P25 TiO_2 was used in this work. The other chemicals and solvents were supplied by Aldrich and Merck. All chemicals were analytical grade and were used as received without any further purification. The working solutions were prepared using analytical grade chemicals and double distilled water. The organic solvents were spectroscopic grade.

2.2. CdS/TiO_2 nanocomposite preparation

Initially, a precursor compound was prepared by the reaction of thiourea ($SC(NH_2)_2$) with cadmium nitrate ($Cd(NO_3)_2 \cdot 4H_2O$) in methanol in 2:1 proportion according to the reaction: $2SC(NH_2)_2 + Cd(NO_3)_2 \cdot 4H_2O \rightarrow Cd[SC(NH_2)_2]_2(NO_3)_2$ [9].

Preparation of mixed composites was performed by impregnating the precursor compound in methanol onto the surface of TiO_2. The mole ratios Cd/Ti = 0.2, 0.05, 0.03 and 0.01 were prepared. Each sample was mixed for 30 min in methanol medium, followed by solvent evaporation under vacuum. After the impregnation, the precursor/TiO_2 composites were thermally treated in a tube under N_2 flow (30 mL min^{-1}) at 10 °C min^{-1} up to 300 °C for 1 h. After thermal treatment the composites were cooled down to room temperature. BET (N_2) surface areas of the samples were 45.00 m^2 g^{-1} for pristine TiO_2, 24.25 m^2 g^{-1} for CdS/TiO_2 1% composite and 23.57 m^2 g^{-1} for CdS/TiO_2 5% composite.

2.3. Photocatalitic procedure

The degradations were carried out using the textile reactive dye Drimaren red (color index 18286). Briefly, 100 mL of aqueous Drimaren red solution (50 mg L^{-1}) was exposed to ultra-violet radiation in the presence of 30 mg of TiO_2 (for pure TiO_2 or CdS/TiO_2 catalysts). The photocatalytic reactor used has a surface area ca. 155 cm^2 illuminated by a low-pressure mercury lamp (output at 254 nm, 15 W) kept at 10 cm distant from the solution. The value of light irradiance was 161 μW cm^{-2}. The reaction was monitored by discoloration measurements with an UV–vis spectrophotometer.

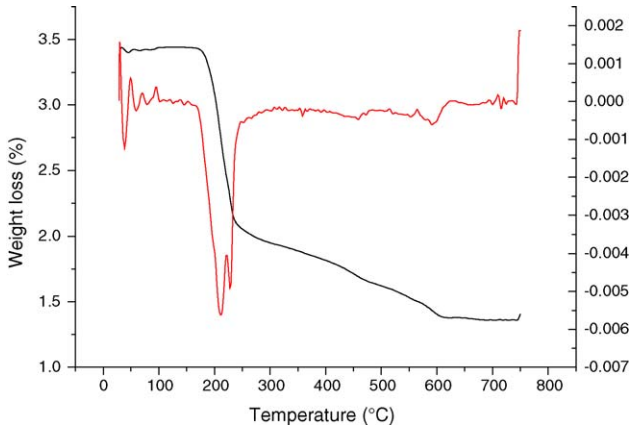

Fig. 1. Thermogravimetric analyzes (TG and DTG) curves of decomposition of $Cd[SC(NH_2)_2]_2(NO_3)_2$.

3. Results and discussion

3.1. Thermogravimetric and XRD analysis

Thermogravimetric analysis were carried out in N_2 atmosphere to investigate the thermal decomposition of the $Cd[(SC(NH_2)_2)_2](NO_3)_2$ precursor; results are shown in Fig. 1. For the pure precursor a weight loss of 45% in the temperature range 34–317 °C and of 17% in the 317–741 °C range were observed. The weight loss for the conversion of the precursor compound $Cd[SC(NH_2)_2]_2(NO_3)_2$ to CdS is 63%, which is consistent with the two main thermogravimetry features, that correspond to 62% weight loss. Similar thermal decompositions, i.e. temperature range, were observed for the precursor/TiO_2 composites with a proportional weight loss relative to the pure precursor. These results indicate that no significant effect is produced by the presence of TiO_2 on the thermal decomposition of the $Cd[(SC(NH_2)_2)_2](NO_3)_2$ compound. Based on these results we choose the temperature of 300 °C for carrying out the thermal decomposition of the precursor/TiO_2 composites and preparing the catalyst material.

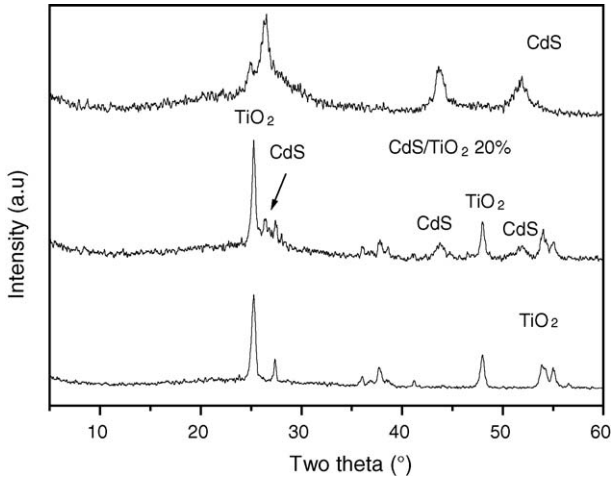

Fig. 2. Powder X-ray diffraction (XRD) pattern of TiO_2, CdS obtained by thermal decomposition of $Cd[SC(NH_2)_2]_2(NO_3)_2$ and of CdS/TiO_2 20% catalyst.

The CdS and CdS/TiO_2 composites were also subjected to X-ray powder diffraction analysis. The XRD profile for TiO_2, CdS and CdS/TiO_2 20% samples are shown in Fig. 2. The XRD profile for the composite provide typical diffraction patterns of hexagonal CdS ($2\theta = 27°$, 44° and 52°) along with peaks due to anatase-TiO_2 ($2\theta = 25°$, 38°, 48° and 54°). Similar patterns were obtained for 1, 3 and 5% CdS/TiO_2 composites. The average size of the CdS/TiO_2 catalyst particles was estimated by analysis of XRD data (considering the anatase-TiO_2 peak) using the Scherrer equation as ranging from 20.7 to 25.2 nm.

3.2. Resonance Raman and laser-induced fluorescence

Resonance Raman scattering can be used to probe the electronic structure of semiconductors due to the strong electron–phonon interaction in these materials [7,22,23]. When studying the behavior of some semiconducting materials such as CdS by means of Raman spectroscopy techniques, one can benefit from the resonance Raman enhancement, which results in more sensitive spectra, when the Raman spectrum is excited with a laser energy resonant to an electronic transition of the material (E_{gap}).

Raman spectra excited at 514.5 nm (2.41 eV) of TiO_2, CdS and CdS/TiO_2 composites prepared at different proportions are displayed in Fig. 3. Strong resonance effect for the CdS phase

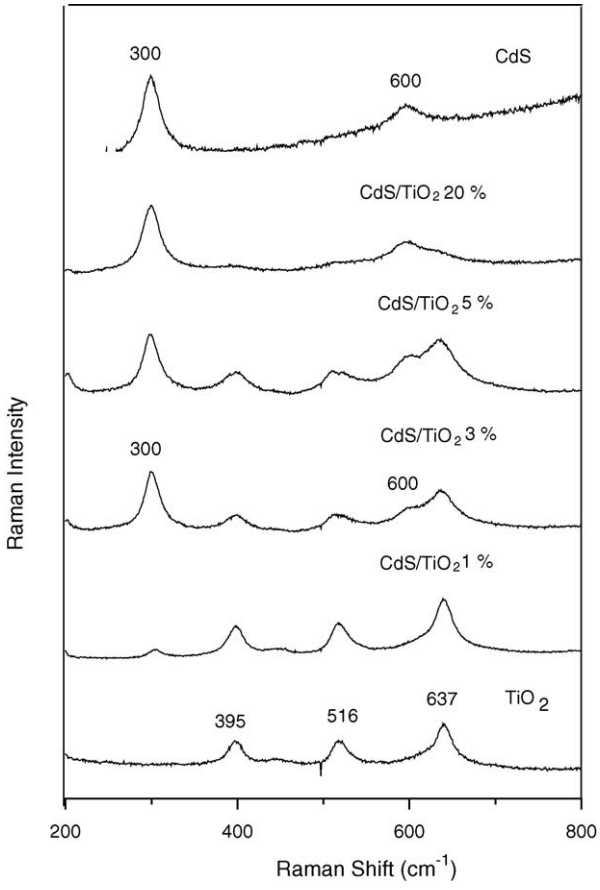

Fig. 3. Raman spectra for TiO_2, CdS and CdS/TiO_2 composites in the 200–800 cm^{-1} range. Laser excitation wavelength at 514.5 nm (E_{laser} = 2.41 eV).

is expected, since the band gap for bulk CdS – 2.42 eV – is very close to the excitation laser energy. Raman spectrum for CdS particles is dominated by an intense band at 300 cm^{-1}, assigned to the first-order longitudinal optic phonon (1 LO) and the second-order LO phonon peak at 600 cm^{-1} [24,25]. The spectra of strongly coupled systems such as CdS are characterized by a vibronic progression in the optical phonon modes, especially at close resonant condition [22]. The TiO_2 spectrum in the 200–800 cm^{-1} region is dominated by the 395, 516 and 637 cm^{-1} bands, characteristic of the TiO_2-anatase phase. A weak feature can be seen at 443 cm^{-1}, indicating the presence of a small amount of rutile modification of TiO_2 [26]. Raman spectra of the composites show a combination of the two semiconducting characteristic bands. With increasing the CdS ratio in the composites, the intensity of the bands assigned to CdS increase proportionally, while the TiO_2 bands decrease progressively.

Fig. 4 shows the resonance Raman effect for the CdS/TiO_2 5% composite. While for TiO_2 modes, no significant spectral changes can be seen upon variation of the laser wavelength, marked changes in relative intensities of Raman features of CdS as a function of excitation wavelength occur. The FT-Raman spectrum (excited at 1064 nm or 1.16 eV) exhibits only prominent peaks due to titania anatase phase. No Raman lines due to CdS are observed. This laser energy is smaller than CdS or TiO_2 bulk band gaps and no significant contribution from resonance Raman effect is expected. At 632.8 nm (E_{laser} = 1.96 eV), a strong fluorescent behavior due to CdS occurs. In spite of the fluorescence, Raman lines from the composite are still visible. Spectrum excited at 514.5 nm (2.41 eV) shows a strong contribution form Raman lines associated to CdS relative to

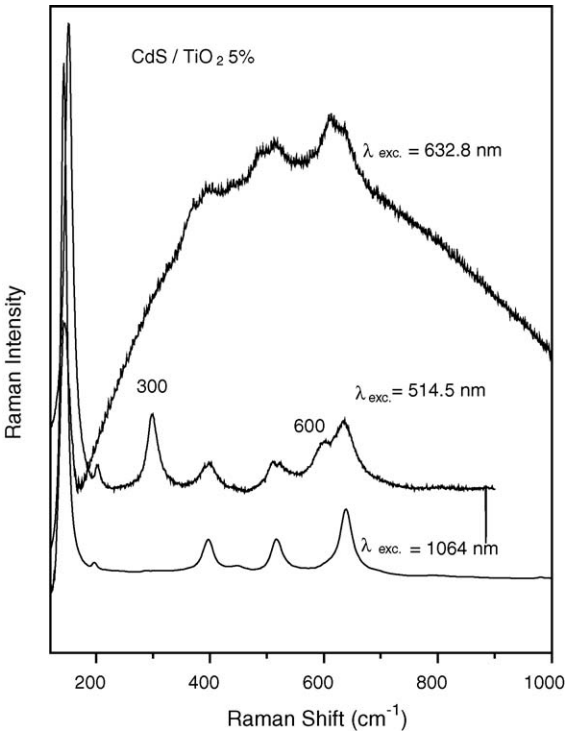

Fig. 4. Raman spectra for CdS/TiO_2 5% catalyst at different laser excitation wavelengths.

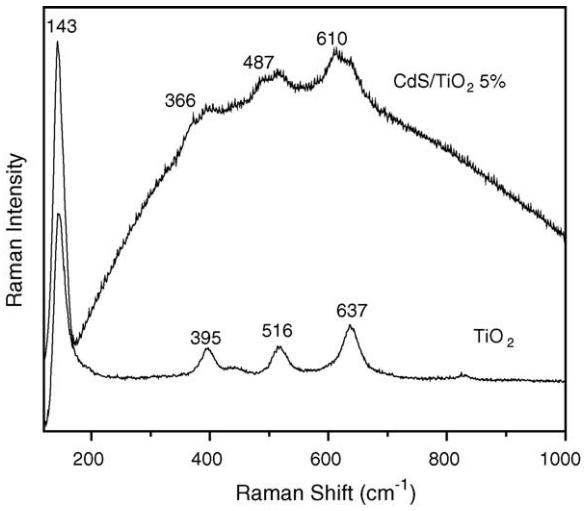

Fig. 5. Raman spectra for TiO_2 and CdS/TiO_2 5% catalyst. Laser excitation wavelength at 632.8 nm (E_{laser} = 1.96 eV).

TiO_2 modes due to strong resonant Raman effect at this laser wavelength.

Fig. 5 compares the Raman spectra of the TiO_2 and CdS/TiO_2 5% samples excited at 632.8 nm (E_{laser} = 1.96 eV). It is very interesting to observe that each TiO_2 phonon mode between 300 and 700 cm^{-1} is split into two components: one at the same frequency as for TiO_2 and a second one at lower wavenumber. The observed frequency separation between split peaks is about 20–30 cm^{-1}: upon interaction with CdS, characteristic TiO_2 bands show a rather large phonon softening from 395 to 366 cm^{-1}, 516 to 487 cm^{-1} and from 637 to 610 cm^{-1}. The phonon modes softening observed for the CdS/TiO_2 composites may be related to a charge transfer between CdS and TiO_2 conductions bands: CdS gives extra electrons to the TiO_2 conduction band (which corresponds to antibonding states). The increase in charge density in the TiO_2 conduction band is reflected in lower energy phonon vibrations for such doped phase. In fact, direct electron transfer between excited CdS and TiO_2 particles has

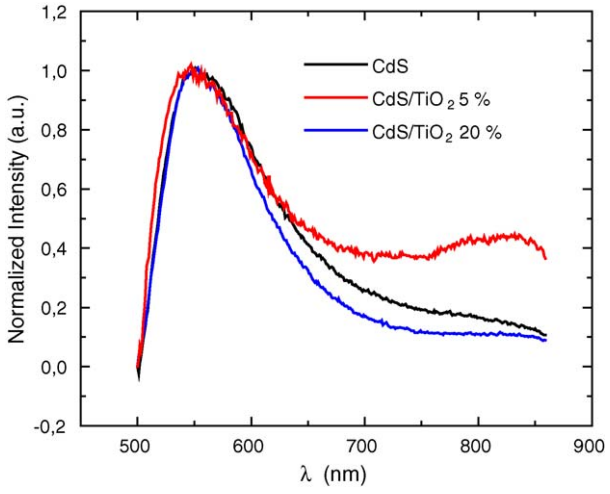

Fig. 6. Laser-induced fluorescence spectra of CdS and CdS/TiO_2 at different molar proportions.

been observed by Sant and Kamat [8] using emission and transient absorption spectroscopy.

Fig. 6 presents the laser-induced fluorescence spectra of CdS and CdS/TiO_2 composites. An intense broad band related to CdS E_{gap} transition is seen at ca. 550 nm. An additional band at lower energies is evident for the CdS/TiO_2 5% catalyst, and probably results from the electronic interaction between TiO_2 and CdS as revealed by the resonance Raman data.

The electronic properties of quantum-sized CdS are dependent on the size of the particles [8]. Thus, absorption or emission spectra may vary depending on specific characteristics of the sample. If a distribution of sizes exists, this may cause a broadening in emission or absorption bands. This could be related to the fact that 632.8 nm laser strongly induces CdS photoluminescent behavior.

3.3. Photocatalityc activity

As the TiO_2 P25 shows a relatively high surface area the reactive dye will significantly adsorb on the photocatalyst surface. To account for this adsorption, before the catalytic tests the dye solution was left in contact with the photocatalyst for 1 h in the dark to reach the adsorption equilibrium. It was observed that the pure TiO_2 can adsorb approximately 8% of the initial dye which was similar to the other composites with 1, 3, 5 and 20%. The color removal of the dye solution by UV irradiation as a function of time was monitored by the absorbance value at the maximum of the absorption spectrum of the dye (523 nm, $\varepsilon = 1.4 \times 10^4\ mol^{-1}\ L\ cm^{-1}$). Although the photooxidation of molecules such as textile dyes are quite complex, the discoloration is directly related to the initial steps of the oxidation process (Eq. (1)) which is followed by consecutive reactions leading to the mineralization of the dye (Eq. (2)):

$$\text{dye} \rightarrow \text{non-colored intermediate (discoloration)} \quad (1)$$

$$\text{non-colored intermediate} \rightarrow CO_2 + H_2O\ \text{(mineralization)} \quad (2)$$

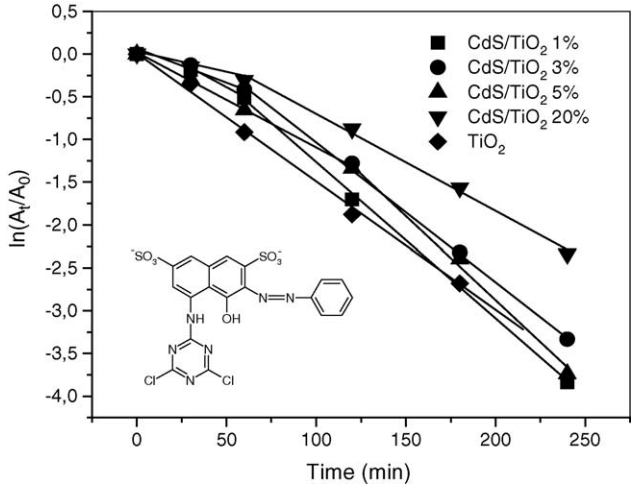

Fig. 7. Photodegradation reaction of organic dye Drimaren red (shown in the insert) in aqueous solution (50 mg L^{-1}) in the presence of TiO_2 and CdS/TiO_2 composites monitored by UV–vis spectroscopy. The TiO_2 loading was 30 g L^{-1} in every case.

Table 1
Comparison of the rate constants (k_2) for Drimaren red photodegradation reaction in the presence of different catalysts

Catalyst	$k_2 \pm 0.001$ (min^{-1})
CdS/TiO_2 1%	0.0184
CdS/TiO_2 3%	0.0163
CdS/TiO_2 5%	0.0200
CdS/TiO_2 20%	0.0122
TiO_2	0.0152

Therefore, the discoloration rate can be used to obtain kinetic information on the photocatalytic process. Fig. 7 shows a plot of $\ln A_t/A_0$ (A = absorbance at 523 nm) versus reaction time; to reasonable approximation, its slope equals the apparent first-order rate constant [2,27,28]. From the plot (Fig. 7), it can be detected that the composites present a more complex kinetic behavior than the TiO_2, from which we derive two velocity constants k_1 and k_2. The reaction starts with a latency period dictated by the velocity constant k_1, followed by the increase in the velocity of the dye degrading reaction, this one characterized by the constant k_2. We considered k_1 for reaction time until 60 min, and k_2 after that. As the dye absorbs in the visible and especially near the E_{gap} of CdS, the sensitization mechanism of photocatalysis is possible in this case. Such a mechanism could explain the complex degradation kinetics (two reaction constants) in the case of CdS/TiO_2 materials. Similar behavior at discoloration rate of Drimaren red at similar experimental conditions was observed for catalysts composites SnS/TiO_2 recently investigated by our group [29]. For the comparison to the degrading rate of pure TiO_2, we have used the k_2 constants. Kinetic parameters are shown in Table 1, and indicate that CdS/TiO_2 1, 3 and 5% composites present a better performance than TiO_2 in the photodegradation reaction of the model dye. On the other hand, in the case of the CdS/TiO_2 20% catalyst, a decrease in the rate constant as compared to plain TiO_2 is observed. It is likely that the sorption of the dye on the catalyst surface is an important step in the decomposition reaction. At higher CdS proportions, affinity between catalyst and dye may decrease, thus affecting the photooxidation reaction rate.

4. Conclusions

A mixed catalyst was prepared aiming to improve photocatalytic properties of TiO_2. CdS/TiO_2 composites were prepared by a method not yet described in the literature, that is, the thermal decomposition of cadmium thiourea impregnated on TiO_2 surface. The obtained material was studied by XRD, laser-induced fluorescence and resonance Raman spectroscopy, which gave information about the structural and electronic characteristics of the nanosized CdS/TiO_2 mixed catalysts. In addition, the capability of coupled CdS/TiO_2 for photocatalytic degradation of an organic textile dye was investigated. In those tests, several composites with different CdS/TiO_2 proportions were compared in terms of their efficiency as catalysts.

Raman spectra are sensitive to variations in charge density which results from chemical interactions, and allowed the study

of electronic interaction between the two associated materials. Presented results point to a lattice softening of the TiO_2-anatase phase due to electronic interaction with CdS in the CdS/TiO_2 catalyst, showing that the composite is not constituted of a mere physical mixture of both components. Moreover, resonance Raman and laser-induced fluorescence experiments clearly show that the electronic interaction is stronger for 5% CdS/TiO_2 proportion.

The obtained results suggested that the most efficient photocatalyst is the CdS/TiO_2 5% composite, since kinetic parameters show that the decomposition rate depends on the CdS load and reaches a maximum at a 5% CdS/TiO_2 proportion. A connection between this fact and the abovementioned electronic interaction between both semiconductors is to be further investigated.

Acknowledgements

This work was partly supported by FAPESP. P. Corio gratefully acknowledges a fellowship from CNPq (307840/2003-4). The authors are also thankful to Instituto do Milênio/Instituto de Nanociências/CNPq and to Dr. Luiz Cury from Departamento de Física/ICEx-Universidade Federal de Minas Gerais for the photoluminescence experiment and to Dr. Rochel M. Lago for useful discussions about photocatalytic tests.

References

[1] M.R. Hoffmann, S. Martin, W.Y. Choi, D.W. Bahnemann, Chem. Rev. 95 (1995) 69–96.
[2] I.K. Konstantinou, T.A. Albanis, Appl. Catal. B: Environ. 42 (2003) 319–335.
[3] V.A. Sakkas, I.M. Arabatzis, I.K. Konstantinou, A.D. Dimou, T.A. Albanis, P. Falaras, Appl. Catal. B: Environ. 49 (2004) 195–205.
[4] S. Somasundaram, N. Tacconi, C.R. Chenthamarakshan, K. Rajeshwar, N.R. de Tacconi, J. Electroanal. Chem. 577 (2005) 167–177.
[5] G. Liu, X. Zhang, Y. Xu, X. Niu, L. Zheng, X. Ding, Chemosphere 55 (2004) 1287–1291.
[6] S. Lo, C. Lin, C. Wu, P. Hsieh, J. Hazard. Mater. 114 (2004) 183–190.
[7] S. Zou, M.J. Weaver, J. Phys. Chem. B 103 (1999) 2323–2326.
[8] P.A. Sant, P.V. Kamat, Phys. Chem. Chem. Phys. 4 (2002) 198–203.
[9] H. Weller, Angew. Chem. Int. Ed. Engl. 32 (1993) 41–53.
[10] J. Bandara, K. Tennakone, P.P.B. Jayatilaka, Chemosphere 49 (2002) 439–445.
[11] R. Vogel, P. Hoyer, H. Weller, J. Phys. Chem. 98 (1994) 3183–3188.
[12] L.M. Peter, D.J. Riley, E.J. Tull, K.G.U. Wijayantha, Chem. Commun. 10 (2002) 1030–1031.
[13] Y. Bessekhouad, D. Robert, J.V. Weber, J. Photochem. Photobiol. A: Chem. 163 (2004) 569–580.
[14] N. Serpone, P. Maruthamuthu, P. Pichat, E. Pelizzetti, H. Hidaka, J. Photochem. Photobiol. A: Chem. 85 (1995) 247–255.
[15] M. Takahashi, H. Natori, K. Tajima, K. Kobayashi, Thin Solid Films 489 (2005) 205–214.
[16] T. Toyoda, K. Saikusa, Q. Shen, Jpn. J. Appl. Phys. Part 1 38 (1999) 3185–3186.
[17] M. Hodos, E. Horváth, H. Haspel, Á. Kukovecz, Z. Kónya, I. Kiricsi, Chem. Phys. Lett. 399 (2004) 512–515.
[18] J.C. Yu, L. Wu, J. Lin, P. Lia, Q. Li, Chem. Commun. 13 (2003) 1552–1553.
[19] N. Tohge, M. Asuka, T. Minami, J. Non-Cryst. Solids 147 (1992) 652–656.
[20] V.C. Costa, F.S. Lameiras, M.T.C. Sansiviero, A.B. Simões, W.L. Vasconcelos, J. Non-Cryst. Solids 348 (2004) 190–194.
[21] B.E. Boone, A. Gichuhi, C. Shannon, Anal. Chim. Acta 397 (1999) 43–51.
[22] A. Gichuhi, B.E. Boone, C. Shannon, J. Electroanal. Chem. 522 (2002) 21–25.
[23] J.J. Shiang, S.H. Risbud, A.P. Alivisatos, J. Phys. Chem. 98 (1993) 8432–8442.
[24] J.M. Nel, H.L. Gaigher, F.D. Auret, Thin Solid Films 436 (2003) 186–195.
[25] B. Schreder, C. Dem, M. Schmitt, A. Materny, W. Kiefer, U. Winkler, E. Umbach, J. Raman Spectrosc. 34 (2003) 100–1003.
[26] T. Stergiopoulos, M. Bernard, A. Hugot-Le Goff, P. Falaras, Coord. Chem. Rev. 248 (2004) 1407–1420.
[27] I.K. Konstantinou, T.A. Albanis, Appl. Catal. B: Environ. 49 (2004) 1–14.
[28] I.M. Arabatziz, T. Stergiopoulos, M.C. Bernard, D. Labau, S.G. Neophytides, P. Falaras, Appl. Catal. B: Environ. 42 (2003) 187–201.
[29] M.T.C. Sansiviero, A.C. Bernardes-Silva, F. Magalhães, R.M. Lago, Book of Abstracts of 13° Congresso Brasileiro de Catálise/3° Mercocat, Foz do Iguaçu/Pr/Brazil 2 (2005) 1180–1183.